Heliyon 10 (2024) e27499

Contents lists available at ScienceDirect

Heliyon

journal homepage: www.cell.com/heliyon

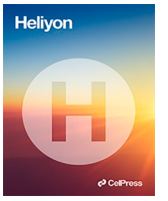

Research article

Green cleanup of styrene-contaminated soil by carbon-based nanoscale zero-valent iron and phytoremediation: Sunn hemp (*Crotalaria juncea)*, zinnia (*Zinnia violacea* Cav.), and marigold (*Tagetes erecta* L.*)*

Ann Kambhu, Tunlawit Satapanajaru *, Piyapawn Somsamak, Patthra Pengthamkeerati, Chanat Chokejaroenrat, Kanitchanok Muangkaew, Kanthika Nonthamit

Department of Environmental Technology and Management, Faculty of Environment, Kasetsart University, Bangkok, 10900 Thailand

A R T I C L E I N F O

Keywords:
Remediation
Styrene
Phytoremediation
Carbon-based materials
Nano zerovalent iron

A B S T R A C T

Accidental chemical spills can result in styrene-contaminated soil. Styrene negatively affects human health and the environment. The objective of this study was to remediate styrene-contaminated soil using a combination of activated carbon-based nanoscale zero-valent iron (nZVI-AC) and phytoremediation by sunn hemp (*Crotalaria juncea*), zinnia (*Zinnia violacea* Cav.) and marigolds (*Tagetes erecta* L.). The results showed that all three plant types could potentially increase the removal efficiency of styrene-contaminated soil. At 28 days, all three plants showed complete removal of styrene from the soil with 1 g/kg of nZVI-AC, activated carbon-based nZVI synthesized by tea leaves (*Camellia sinensis*) (T-nZVI-AC), or activated carbon-based nZVI synthesized by red Thai holy basil (*Ocimum tenuiflorum* L.) (B-nZVI-AC). However, styrene removal efficiencies of sunn hemp, zinnia, and marigold without carbon-based nZVI were 30%, 67%, and 56%, respectively. Statistical analysis (ANOVA) revealed that the removal efficiencies differed significantly from those of phytoremediation alone. With the same removal efficiency (100%), the biomass of sunn hemp in nano-phytoremediation treatments differed by approximately 55%, whereas the biomass of zinnia differed by >67%, compared with that of the control experiment. For marigold, the difference in biomass was only 30%. Styrene was adsorbed on surface of soil and AC and then further oxidized under air-water-nZVI environment, while phytovolatilization played an important role in transporting the remaining styrene from the contaminated soil to the air. Marigold was used as an alternative plant for the nano-phytoremediation of styrene-contaminated soil because of its sturdy nature, high biomass, tolerance to toxic effects, and ease of cultivation. Remediation of one cubic meter of styrene-contaminated soil by a combination of carbon-based nanoscale zero-valent iron and phytoremediation by marigolds emitted 0.0027 $kgCO_2/m^3$.

* Corresponding author.
E-mail address: fscitus@ku.ac.th (T. Satapanajaru).

https://doi.org/10.1016/j.heliyon.2024.e27499
Received 12 December 2023; Received in revised form 29 February 2024; Accepted 29 February 2024
Available online 7 March 2024

1. Introduction

Styrene is the primary material used in the production of fiberglass, plastics, polyesters, resins, and rubber. Furthermore, styrene is potentially carcinogenic to humans (Group 2A) [1]. Additionally, the Toxics Release Inventory has reported that styrene ranks 15 out of 531 toxic chemicals. In 2021, 33.5 million pounds of styrene was released into the environment; approximately 92% was released into the air, 7% through off-site disposal or other releases, and 1% on the land [2]. Styrene is often found in topsoil due to its high percentage of organic carbon [3]. The organic carbon-water partition coefficient (K_{oc}) of styrene is high (260), which means that styrene is likely to remain in the soil [4].

Many physical, chemical, and biological remediation methods are available for removing organic pollutants, including styrene, from contaminated soil [5]. However, these methods have one or more limitations. Styrene treatment has been studied for several decades. A pioneering study on styrene biodegradation in aquifer materials was conducted in 1992. The first study on the biodegradation of styrene in aquifer materials by Fu and Alexander in 1992 showed that styrene could be easily transformed under aerobic conditions [6]. Recently, other researchers have found similar results showing that styrene can be easily degraded by bacteria or other microorganisms under aerobic conditions [7]; however, if styrene is present under anaerobic conditions, the degradation rate is reduced [8]. Using plants to remove pollutants from the environment (phytoremediation) is an economical and ecologically friendly approach that can be used immediately in contaminated areas. Other remediation techniques are expensive, consume large amounts of energy, and use large amounts of chemicals. Most importantly, waste can be generated during the remediation process. The placement of flowering and ornamental plants also improves the scenery in the treated area. Additionally, some plants can be used as animal feed. Alfalfa is a perennial flowering plant of the legume family that has been studied for the remediation of contaminated land. This can help increase the number of rhizospheres in the soil [9]. Additionally, remediation of soil contaminated with polycyclic aromatic hydrocarbons with a combination of alfalfa and *Rhizobium meliloti* showed that the concentration decreased by 51.4% after 90 days [10]. For chemical remediation, nanoscale zero-valent iron (nZVI) 1–100 nm in size is an effective material for remediating contaminated soil [11]. Reductive transformation using nZVI is a simple and successful remediation method [12]. Owing to its small size, large specific surface area, and high surface reactivity, nZVI has a high potential for donating electrons to destroy the chemical structure of organic pollutants. Over the past decade, several studies have demonstrated that nZVI can successfully transform many organic pollutants. Presently, the study of the combination of nanotechnology and phytoremediation for remediating organic pollutant-contaminated soil, such as chlorfenapyr (pesticide), is called nano-phytoremediation. These processes require nanoparticles or nanomaterials that are safe for plants, promote plant growth and root spreading, increase plant enzymes, and accelerate the removal of contaminants [13]. The results indicated that the combination of both methods enhanced the removal efficiency of contaminated soil remediation. Due to environmental concerns, the use of green-synthesized nanoparticles is one of the best alternative materials that is safe for plants.

Currently, green synthesis of nanoparticle from plant extracts is widely used due to its overcome the unfavorable impacts of their production via chemical routes [14], such as, the synthesis of nZVI (Fe^0) from broadleaf plantain (*Plantago major* L.) [15], Au^0 from Aloe vera [16], and Zn^0 from neem (*Azadirachta indica*) [17]. Furthermore, the green synthesis of nanoparticles from plant extracts is preferred over other extraction methods because it is cost-effective, nontoxic, widely available, and environmentally friendly. It can be used for various purposes, such as medicine, environmental treatment, bioengineering sciences, and biotechnology [18].

The green-synthesized nZVI stands out due to its small size, large surface area, high reactivity, and magnetic properties. These features make it effective in removing various pollutants, both inorganic and organic compounds in soil and water, such as, removal of methylene blue dye (MB) from aqueous solution using nZVI produced from (*Ricinus communis)* seeds extract [14], or remediating Cr^{6+} in chromium slag dump sites using a green tea-derived nanoscale zero-valent iron/nickel (GT-nZVI/Ni) [19]. In addition, using supporting materials for nZVI, carbon-based materials such as activated carbon (AC), biochar, carbon nanotubes, and graphene, which provide a large specific surface area and porous structure, can enhance remediation efficiency [11]. Zhu et al. (2020) successfully synthesized a biochar-supported nano zero-valent iron/nickel bimetallic composite (BC@nZVI/Ni) to activate persulfate (PS) for the degradation of norfloxacin (NOR) in water [20]. Rashtbari et al. (2022) developed nZVI incorporated on activated carbon (AC/nZVI) for removal of furfural, an organic in nature, considered a pollutant having a toxic effect on humans and their environment. The results showed that AC/nZVI was efficient and inexpensive t to eliminate furfural from a liquid solution [21].

The objective of the current study was to enhance phytoremediation efficiencies for styrene-contaminated soil by carbon-based nZVI and by sunn hemp (*Crotalaria juncea*), zinnia (*Zinnia violacea* Cav.) and marigolds (*Tagetes erecta* L.), These local tropical plants have been selected from root systems that promote microbial growth and grow well in the hot climate of Thailand. Marigold and zinnia are flowering plants that provide aesthetically pleasing scenery, whereas sunn hemp is used as animal feed. The nZVI used in this study was green-synthesized from the leaves of red Thai holy basil (*Ocimum tenuiflorum* L.) (B-nZVI) and tea leaves (*Camellia sinensis*) (T-nZVI), which are environmentally friendly. Implementation of a combination of various remediation techniques can be essential in land reclamation.

2. Material and methods

2.1. Materials

Commercial ZVI powder (purity 99%) was purchased from S.D. Fine Chem, Ltd. (particle size: <100 mesh). Ferric chloride ($FeCl_3{\cdot}6H_2O$) was obtained from Ajax. Sodium borohydride ($NaBH_4$) was purchased from Asia Pacific Specialty Chemicals, Ltd. Hydrochloric acid (HCl) was purchased from J.T. Baker. Sodium hydroxide (NaOH) was purchased from Carlo Erba Reagent. Methanol

was purchased from Merck. The styrene analytical standard was obtained from Sigma-Aldrich. Acetonitrile (99.9%) was from RCI Labscan and formic acid (85%), was purchased from Qrec.

2.2. Preparation and characterization of green-synthesized nZVI

The nZVI particles were synthesized by adding a 1:1 vol ratio of $NaBH_4$ (0.25 M) to $FeCl_3$ (0.045 M) (Satapanajaru et al., 2011). The solutions were mixed at room temperature for 5 min. Ferric iron was reduced by borohydride to generate nZVI. Green-synthesized nZVI (T-nZVI and B-nZVI) was prepared according to the method described by Romeh and Saber (2020). Twenty grams of dried tea leaves (*C. sinensis*) or red Thai holy basil leaves (*O. tenuiflorum* L.) was briefly heated to 80 °C in 1.0 L of deionized water and filtered using a vacuum filter. Then, 0.1 M $FeCl_3$ was added to 20 g of the dried material. Subsequently, the green extracts of both tea and red basil were mixed with the adsorbents and $FeCl_3$ in a 1:2 ratio (v/v) and stirred for 1 h. The mixture was precipitated by centrifugation at 5000 rpm for 30 min. The wet paste was then placed in an oven at 60 °C overnight. AC (commercial grade) was added to the nZVI suspension solution, and processing was conducted with constant stirring using a magnetic stirrer for 2 h. The nZVI-AC particles were separated by centrifugation (Centurion, Model 1000 Series) at 5000 rpm for 5 min. Finally, the precipitate was collected and washed once each with deionized water and ethanol. The resulting precipitate was dried at 80 °C for 6 h in a hot-air oven (Memmert, Model 30–750).

To investigate the physical and morphological characteristics of AC and nZVI-AC, the BET surface area method was applied using Quantachrome: Autosorb-1. The sizes and shapes of the nZVI and nZVI-AC particles were determined using scanning electron microscopy with energy-dispersive X-ray spectroscopy (SEM/EDX) and transmission electron microscopy (TEM; JEOL: JEM1220). An X-ray diffractometer (XRD; Philips X'Pert) was used to investigate the material structures of all the types of nZVI.

2.3. Removal of styrene from water and soil by nZVI-AC and green-synthesized nZVI-AC

Batch experiments were conducted to examine the styrene-removal efficiencies of nZVI-AC, T-nZVI-AC, and B-nZVI-AC. Styrene solutions were prepared in deionized water at initial concentrations of 2.5, 5, 7.5, and 10 mg/L. The solution (100 mL) was poured into a 250 mL Erlenmeyer flask, and 1 g/L of each nZVI-AC was added and capped. The flasks were shaken on a rotating shaker at 150 rpm. The experiment was performed in triplicate at room temperature. The samples were collected at a pre-selected time of 24 h. The samples were centrifuged at 13,000 rpm for 5 min. The residual concentrations of styrene were quantified using high-performance liquid chromatography (HPLC; LC-20-A, SPD, Shimadzu, Japan) using acetonitrile (ACN) and deionized water (70:30 v/v) as the mobile phase with a C18 (Cosmosil 5C18-MS-II, 5 μm, 150 mm × 4.6 mm) column under a flow rate of 1.0 mL/min. The change in the amount of styrene before and after the treatment with nZVI-AC was quantified. The styrene intermediate and by-products were separated using the LC-MS 1200 infinity series (6490 Triple Quadrupole LC-MS Systems) with a Zorbax SB-C18 (2.1 × 150 mm) column at a flow rate of 0.1 mL/min with 20 μL injection volume. The mobile phase was a gradient of 70:30 (ACN: H_2O mixed with 0.1% formic acid; 10 min), 10:90 (5 min), and 100:0 (~30 min). The degradations of the mass of styrene were confirmed using mass spectra obtained from an ion trap mass spectrometer fitted with an electron spray interface (3.5 kV) operated in positive ionization mode at a capillary temperature of 200 °C.

Soil was collected from the central part of Thailand, 20 cm below the soil surface. The soil was air-dried and sieved (dia. <3 mm) beforehand milling. The particle size distribution was determined using hydrometer techniques (American Society for Testing and Materials, 1998; Method D422-63). The percentage of soil organic matter was determined using standard methods [22]. Cation exchange capacity was analyzed using the method of Rhoades (1982) [23]. The characteristics of the clean soil and styrene contaminated soil used in this research were presented in Table S1. The soil was spiked with styrene to an initial concentration of 5 mg/kg. Styrene adsorbed on the soil particles was extracted using ACN with the aid of a sonic disruptor to determine the percent recovery. The sonic disruptor bombarded the soil with sonic waves, facilitating the transfer of soil into the ACN. After 12 h, aliquots were removed and transferred to 1.5 mL microcentrifuge tubes for HPLC analysis. Verification tests showed that >90% of styrene was recovered. Styrene removal experiments were also conducted. The 0.05% and 0.1% (w/w) of normal size nZVI, nZVI-AC, T-nZVI-AC, or B-nZVI-AC were added to prepared styrene contaminated soil. Soil samples from each treatment were collected on days 0, 7, 14, 21, and 28. The changes in the amount of styrene in the soil were investigated.

2.4. Bioassay test for toxicity of styrene on sunn hemp (C. juncea), zinnia (Z. violacea Cav.), and marigolds (T. erecta L.)

A study was conducted to determine the phytotoxic effect of styrene on seed germination, root length, and germination index of sunn hemp (*C. juncea*), zinnia (*Z. violacea* Cav.), and marigolds (*T. erecta* L.). Ten seeds from each plant were sown in each dish with different concentrations of styrene solution (10, 25, 50, 75, and 100 mg/L), with three replicates per treatment. All dishes were incubated in the dark at room temperature for 72 h. The germinated seeds were counted, and the root lengths of the plants were measured. Relative seed germination (RSG), relative root elongation (RRG), and germination index (GI) were calculated as percentages according to Zucconi (1981) using Eqs (1)–(3):

$$RSG\ (\%) = \frac{\text{no. of seeds germinated in the aqueous extract}}{\text{no. of seeds germinated in the control}} \times 100 \quad (1)$$

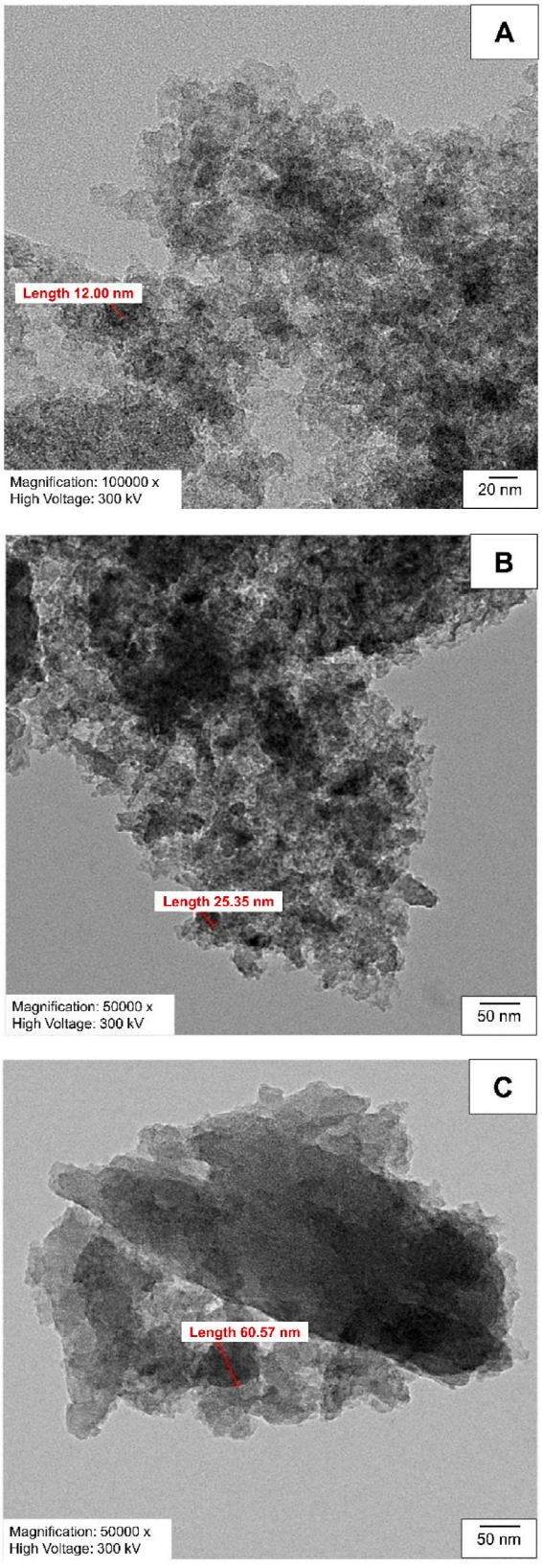

Fig. 1. TEM scanning images of nZVI (A), T-nZVI (B), and B-nZVI (C) nanoparticles.

$$RRG\ (\%) = \frac{\text{mean root length in aqueous extract}}{\text{mean root length in control}} \times 100 \quad (2)$$

$$GI = \frac{\text{seed germination } (\%) \times \text{root elongation } (\%)}{100} \quad (3)$$

Data were analyzed using ANOVA and Tukey's post-hoc test to compare the effects of sample type and concentration level on RSG, RRG, and GI.

2.5. Plant growth test and nano-phytoremediation

Growth and flower quality of sunn hemp (*C. juncea*), zinnia (*Z. violacea* Cav.), and marigolds (*T. erecta* L.) and their responses to different styrene concentrations in the soil were determined. The seeds were allowed to germinate until they had three to four true leaves, which were then transplanted into pots containing styrene-contaminated soil (5 mg/kg). Then, nZVI-AC, T-nZVI-AC, or B-nZVI-AC (0.05–0.1% (w/w)) was added to each pot. Soil samples from each treatment were collected on days 0, 7, 14, 21, and 28. The changes in the amount of styrene in the soil were investigated. After a growth cycle of 35 days after transplanting, morphological observations were performed to determine plant height, number of leaves per plant, number of branches, number of flowers, flower diameter, and flower fresh weight. Cross-sections of the roots, stems, and leaves of each plant exposed to styrene-contaminated soil were also investigated using a microscope. The experiments were performed at ambient temperatures in the range of 24–29 °C.

3. Results and discussions

3.1. Green synthesis of nZVI

The morphologies and sizes of nZVI, T-nZVI, and B-nZVI were investigated using TEM. The TEM images are shown in Fig. 1. At a magnification of × 50,000, it was confirmed that most particles had an average size <100 nm, nZVI (an average size of 12–28 nm and an average surface area of 82–100 m^2/g) (Fig. 1A), T-nZVI, (an average size of 26–37 nm and an average surface area of 40–86 m^2/g) (Fig. 1B), and B-NZVI (average size of 60–80 nm and an average surface area of 10–36 m^2/g) (Fig. 1C). The morphology of both nZVI

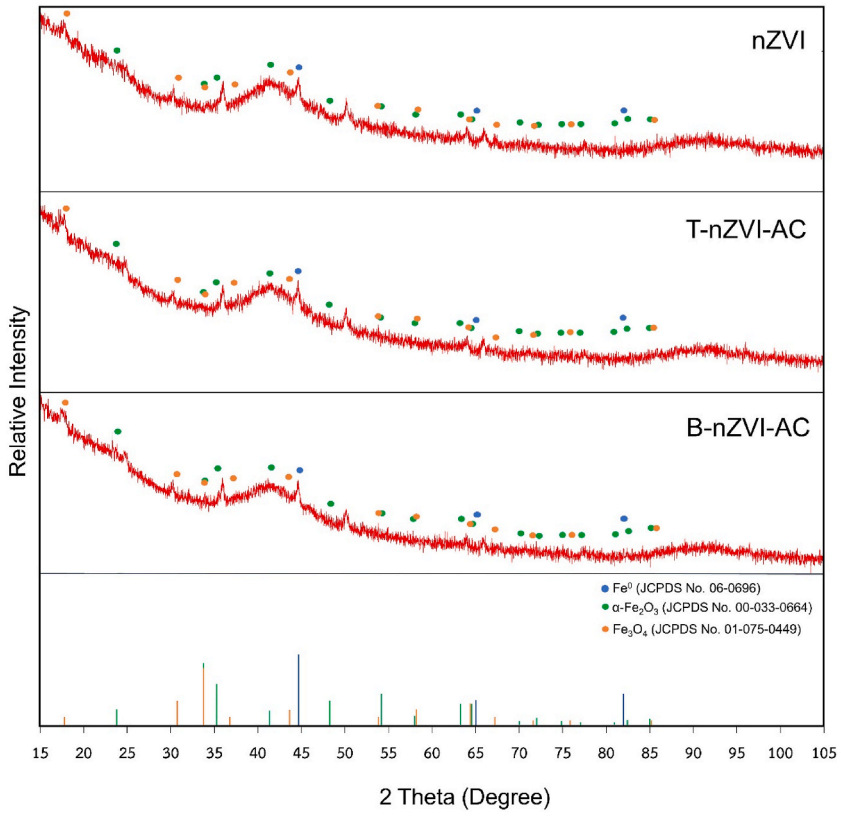

Fig. 2. XRD patterns of green synthesized nZVI, JCPDS stands for Joint Committee on Powder Diffraction Standards). (For interpretation of the references to colour in this figure legend, the reader is referred to the Web version of this article.)

particles was rough, with an aggregated round shape. The same morphological characteristics of nZVI were observed by Satapanajaru et al. (2011) [24] and Romeh and Saber (2020) [13]. The shapes of the green-synthesized nZVI particles were likely due to the distinct reaction times and the complexity of the extract composition [25]. T-nZVI and B-nZVI exhibited a spherical shape along with some irregular shapes and had a form chain-like aggregate. The same results were observed by Abdelfatah et al. (2021) when nZVI was synthesized by plant seeds (*Ricinus communis)* extract [14]. In general, most nanoscale particle sizes in a chain provide a high specific

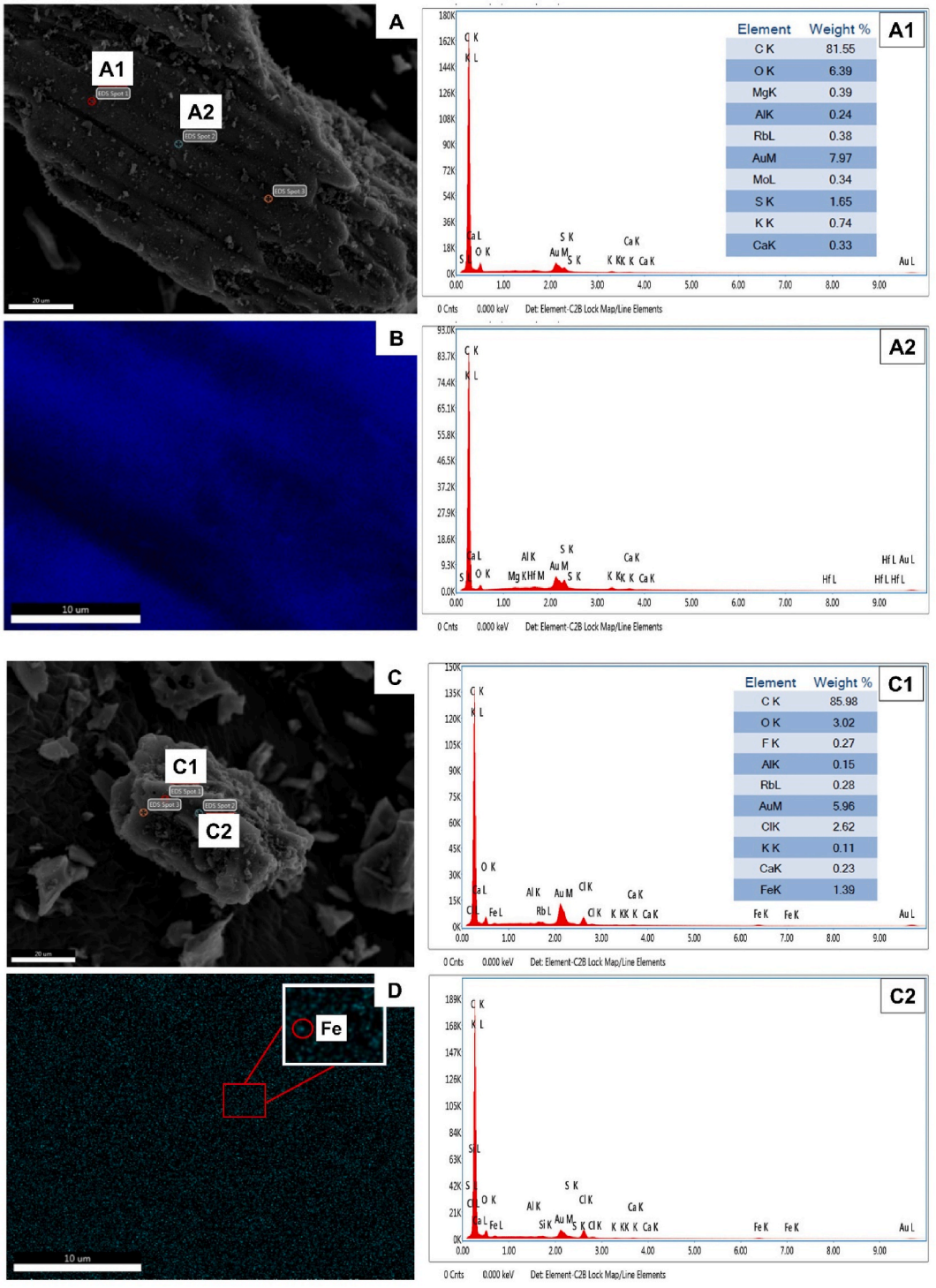

Fig. 3. SEM and EDX images of AC (A and B) and nZVI-AC (C and D).

surface area and reactivity with contaminants [26]. The TEM images show that all the nZVIs are covered by a transparent layer. Abdelfatah et al. (2021) and Saif et al. (2016) indicated that this layer serves as a capping and stabilizing agent to prevent the agglomeration of nZVI and is crucial in improving its dispersion and stability as a basic constituent of green-synthesized nZVI [14,27].

Green synthesis of nZVI by plants is preferred because of the single-step biosynthesis procedure, elimination of hazardous materials, and presence of natural capping agents [28]. In this study, nZVI was green-synthesized from tea leaves (*C. sinensis*) (T-nZVI) and red Thai holy basil (*O. tenuiflorum* L.) (B-nZVI). The XRD patterns of nZVI, T-nZVI, and B-nZVI are shown in Fig. 2. The XRD results show that the strong peak at 44.5°, corresponding to the plane, represents ZVI. This characteristic peak at $2\theta = 44.5°$ was attributed to the cubic-phase structure of nZVI (Abdelfatah et al., 2021). Moreover, the diffraction peak represented high intensities at $2\theta = 41.7°$, corresponding to the α-FeOOH plane. Li et al. (2017) reported that α-FeOOH was the shell layer of ZVI nanoparticles. The current results confirmed that the three types of nZVI were nZVI.

To avoid the agglomeration of nZVI and enhance remediation efficiency, all types of nZVI were embedded in AC. The images of AC (Fig. 3A and B) and nZVI-AC (Fig. 3C and D) were obtained using SEM/EDX. Compared to the porous and smooth texture of AC, the surface of nZVI-AC was characterized by irregular wrinkles with tiny particles, which may have been nZVI deposits. The doped nZVI particles were uniformly distributed on the AC surface and were small, without agglomeration. EDX mapping images in Fig. 3D confirmed the distribution of nZVI on the surface of the AC with 1.39 % by wt (Fig. 3C1–3C2). compared to Fig. 3A1-3A2 and Fig. 3B which shows no deposit of Fe particles on the surface of the AC. The BET results revealed that the special surface area of the AC was 542.27 m^2/g when nZVI had been loaded onto the AC, leading to a significant decrease in the specific surface area to 240.1 m^2/g. This is because the pores on the surface of the AC were filled with nZVI particles. The same results were observed when nZVI particles were coated on sand, silica, silica oxide, and biological sludge [24].

3.2. Treatment of styrene in water and soil by green-synthesized nZVI

Styrene in deionized water (2.5 and 5 mg/L) was treated with 1 g/L nZVI, nZVI-AC, T-nZVI-AC, or B-nZVI-AC, Fig. 4A and B respectively. Fig. 4A showed that T-nZVI-AC and B-nZVI-AC could completely treat styrene within 48 h with 1st order rates (k_{obs}) of 0.0183 and 0.0184 hr^{-1}, respectively. Additionally, nZVI-AC completely treated the styrene within 72 h. However, the styrene removal percentage with nZVI alone was <40. Additionally, Fig. 4B shows that T-nZVI-AC and B-nZVI-AC were able to completely treat styrene within 48 h with 1st order rates of 0.0295 and 0.0296 hr^{-1}, respectively, while the percentage removal of styrene with nZVI was

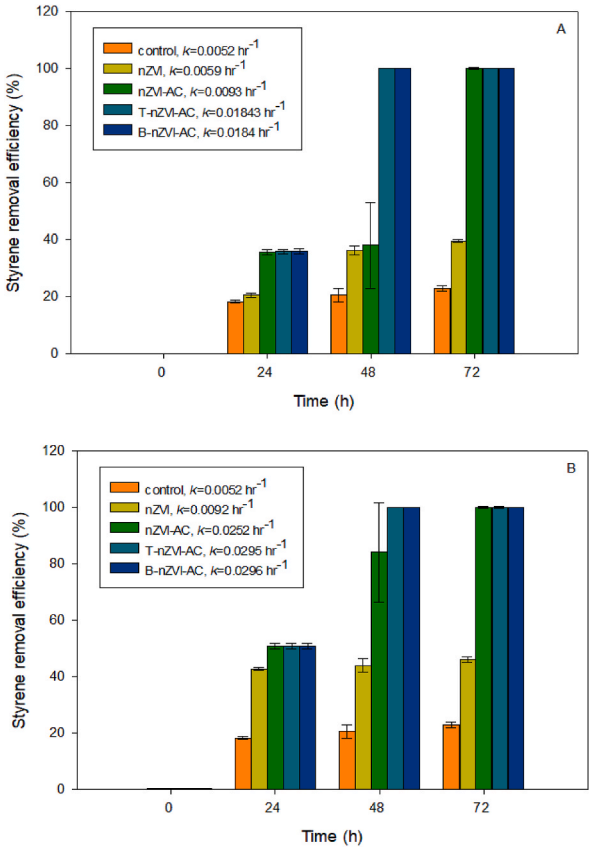

Fig. 4. Removal of 2.5 (A) and 5 (B) mg/L styrene solution with 1 g/L nZVI, nZVI-AC, T-nZVI-AC, and B-nZVI-AC in 72 h.

approximately 40. Even though, the styrene can be degraded on its own, the treatments with all the nZVI-AC give the faster degradation. Mortazavian et al. (2018) immobilized nZVI particles on AC (AC/nZVI) using a two-step synthesis procedure and applied it for the simultaneous adsorption and reduction of contaminants from aqueous solutions [29]. When carbon-based materials and nZVI are used simultaneously, a synergistic effect occurs, promoting the adsorption of pollutants onto the surface of nZVI-AC [11,30]. The results of this study indicate that the maximum concentration of styrene adsorbed on AC without embedded nZVI was 29.46 mg/kg. Styrene was then reduced by nZVI on the AC surface. nZVI plays an important role in donating electrons and generating hydrogen gas owing to its rapid dissolution [31]. The catalytic reduction of styrene under these conditions afforded ethylbenzene [32]. The transformation of organic contaminants is enhanced by NZVI particles, mainly because of the higher surface-area-to-volume ratio [24]. During styrene degradation, nZVI is oxidized to ferrous and ferric ions, and ferrous oxide is formed. Tarekegn et al. (2021) reported that, under actual conditions, nZVI may be covered with an oxide layer [33]. According to the core–shell model theory, the iron oxide shell is largely insoluble under neutral pH conditions and may protect the nZVI core from rapid oxidation. Moreover, surface oxides may be important for styrene adsorption [34]. Previous studies have shown that the reaction rate can shift depending on the initial contaminant concentration, which is presumably due to the saturation of the ZVI-reactive surface sites [35]. The analysis with LC-MS found that the degradation products of styrene ($m/z = 104$) with nZVI-AC possibly were styrene oxide ($m/z = 118$) and 1-phenylethane-1,2-diol ($m/z = 136$) (Fig. 5). The nZVI particles were oxidized to Fe^{2+}, then under aerobic condition, oxygen was accepted an electron and generated hydroxyl radicals ($OH^{\bullet}$). The primary oxidation product of styrene by $OH^{\bullet}$ radicals under Fe^{2+} as a catalyst was styrene oxide which then further oxidized to 1-phenylethane-1,2-diol. Additionally, Xie et al. (2018) have mentioned that the styrene oxide was also further oxidized to benzaldehyde under Fenton-like oxidation [36]. Oliveira et al. (2017) found that the styrene oxidation products were benzaldehyde, acetophenone, ethylbenzene, 2-phenyl ethanol, 2-phenyl acetic acid, 2-phenyl [37]. The proposed mechanism between nZVI-AC and styrene is shown in Fig. 6. There are two mechanisms involved in the reactions between nZVI-AC and styrene; adsorption of styrene on the surface of AC and iron oxides shell, and indirect oxidation of styrene via nZVI.

The treatment of styrene-contaminated soil (5 mg/kg) with 0.5 g/kg of nZVI, nZVI-AC, T-nZVI-AC, or B-nZVI-AC showed that all treatments had similar removal efficiencies; approximately 46%, 54%, 58%, and 62% of styrene removal, respectively, was removed after 28 days (Fig. 7A). When the treatment was increased to 1 g/kg, approximately 61%, 62%, 63%, and 62%, respectively, was removed (Fig. 7B). Statistical analysis (ANOVA) demonstrated that the removal efficiency did not significantly differ among the treatments with 1 g/kg of nZVI-AC, T-nZVI-AC, and B-nZVI-AC ($p < 0.05$). The accelerated removal of styrene with different carbon-based nZVI dosages can be attributed to an increase in the number of surface-active sites. Therefore, a higher dosage favored the removal efficiency of styrene from the soil. Notably, the removal efficiency of styrene in soil was less than that in water, which may be because styrene is incorporated into the humic matter in soil. Moreover, styrene molecules may oligomerize or polymerize spontaneously under aerobic conditions, and clay minerals, such as kaolinite and montmorillonite, may catalyze the polymerization of styrene in soil [6]. The results indicated that the styrene adsorbed on the soil was 26.55 mg/kg (Table S3). Based on the estimated organic carbon partition coefficient (%Organic carbon = 1.59%, Koc = 407.38), the mobility of styrene in soil was considered to be moderate. McCall et al. (1981) reported that the organic carbon partition coefficient of styrene in soil is approximately 370, and styrene is also considered to have moderate mobility in soil [38]. In the control experiment, on day 28, approximately 75% of styrene remained in the soil, and 25% was removed due to volatilization. Styrene rapidly volatilizes from the soil surface but more slowly from deeper strata. In addition, styrene can be biodegraded in soil and sediment with a half-life of 30 and 300 days, respectively [39]. Generally, volatilization and biodegradation of styrene occur simultaneously; however, the main loss mechanism in the soil at certain depths below the surface is probably microbial, providing conditions that favor biological activity [40].

3.3. *Effects of styrene on seed germination and selection of plant for nano-phytoremediation*

Seed germination tests of sunn hemp (*C. juncea*), zinnia (*Z. violacea* Cav.), French marigold (*Tagetes patula* L.), marigold (*T. erecta*

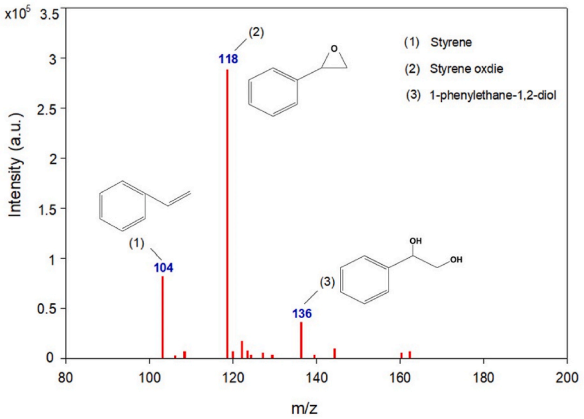

Fig. 5. Mass spectra of styrene and intermediate of styrene from the treatment of styrene by nZVI-AC.

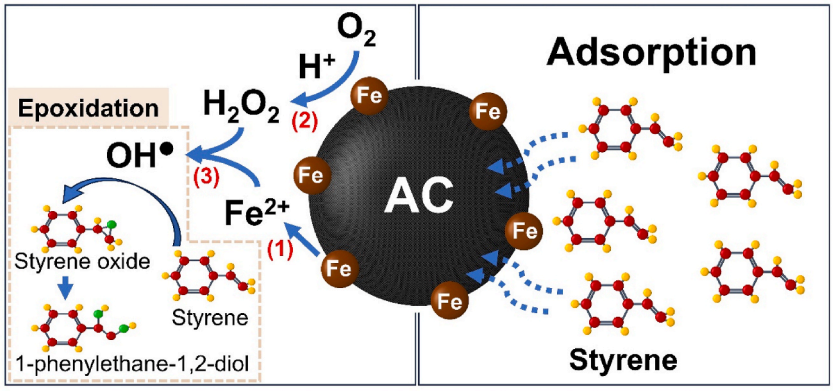

Fig. 6. Proposed mechanism of the treatment of styrene by nZVI-AC in aqueous solution, (1) reduction of Fe, (2) oxidation of oxygen, and (3) Fe^{2+} catalyzation.

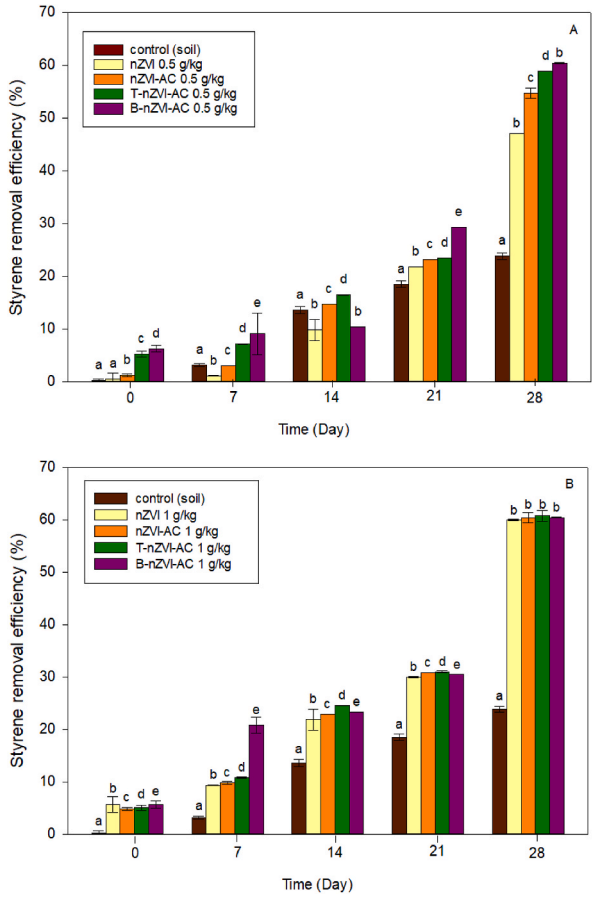

Fig. 7. Removal of 5 mg/kg styrene-contaminated soil using nZVI, nZVI-AC, T-nZVI-AC, and B-nZVI-AC.

L.), and narrowleaf zinnia (*Zinnia angustifolia* Kunth) were conducted by growing 10 seeds of each type in styrene at concentrations of 10 (low), 25, 50, and 75 (high) mg/L over 96 h at room temperature in a dark environment. Fig. 8 shows the RSG of the five plants for the phytoremediation of styrene, and the plant root physiology is shown in Fig. S1. Statistical analysis (ANOVA) revealed that all concentrations significantly affected seed germination of zinnia and narrowleaf zinnia ($p < 0.05$). The seed GI ranges of sunn hemp, zinnia, French marigold, marigold, and narrowleaf zinnia were 90.00–93.94, 70.5–99.47, 32.59–41.81, 99.72–100.00, and 48.78–83.11 %, respectively (Fig. S2). Sunn hemp, zinnia, and marigold showed high seed germination and root elongation and formed a fibrous root system in styrene at all five concentrations. However, French marigold and narrowleaf zinnia showed lower seed

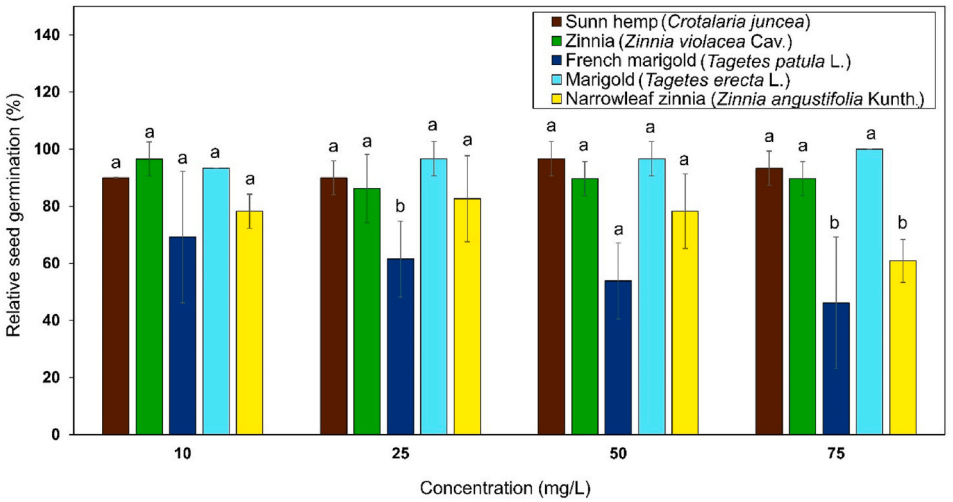

Fig. 8. Relative seed germination of five plants for phytoremediation of styrene at 96 h.

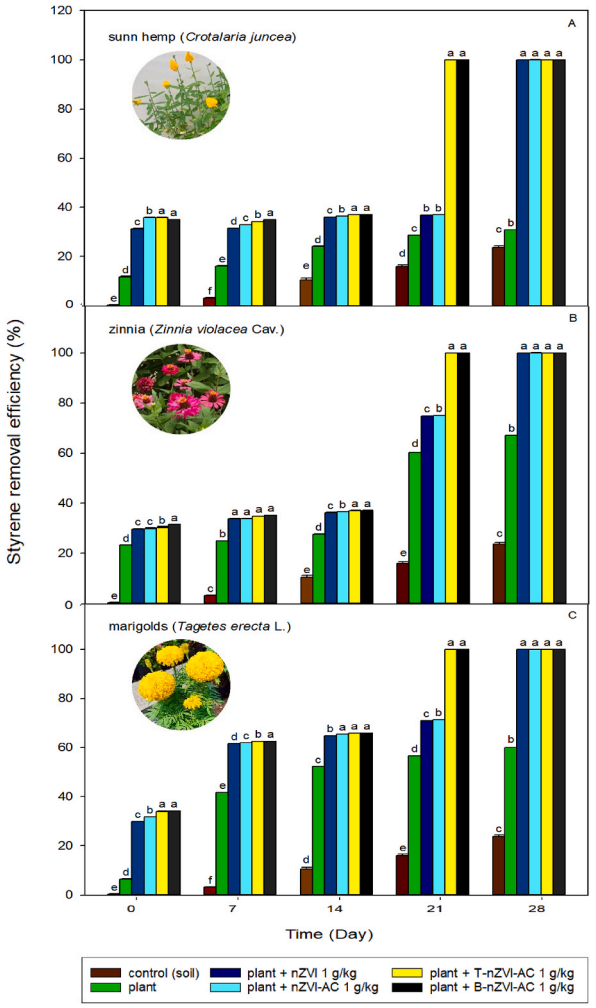

Fig. 9. Nano-phytoremediation of styrene in soil with marigolds (*Tagetes erecta* L.), sunn hemp (*Crotalaria juncea*), and zinnia (*Zinnia violacea* Cav.).

germination <80 % in styrene all concentration in this study (10–75 mg/L). This indicated that French marigold and narrowleaf zinnia were less resistant (GI < 80) to the toxic effects of styrene, even at the lowest tested concentrations (10 mg/L). Henner et al. (1999) revealed that the roots of plants grown in contaminated soils were markedly smaller and more branched than those grown in agricultural soils, which is a typical indicator of chemical toxicity. High quantity of organic and inorganic materials in solution inhibited the germination of plants because these chemicals may change the osmotic pressure outside the seed, decrease water absorption by the seed, and subsequently inhibit seed germination [41]. Moreover, styrene vapor can also inhibit plant germination and development [42]. Mañas and De las Heras (2017) indicated that GI is the most sensitive parameter used to evaluate the toxicity of a residue phytotoxicity dose to seedlings, with a GI value ≥ 80 % indicating no phytotoxicity, or whether substances are present at very low concentrations [43]. Previous research has revealed that suitable plant species for phytoremediation purposes should be strong in nature, have high biomass, be tolerant to toxic effects, be easy to cultivate, have high absorption capacity, and be non-attractive to herbivores [44–47]. Therefore, sunn hemp, zinnia, and marigold were selected for the nano-phytoremediation of styrene-contaminated soil.

3.4. Nano-phytoremediation

Styrene-contaminated soil was treated with 1 g/kg of nZVI, nZVI-AC, T-nZVI-AC, or B-nZVI-AC, followed by sunn hemp, zinnia, or marigold. The results showed that all three plant types had the potential to increase the removal efficiency of styrene-contaminated soil (Fig. 9A–C). After 28 days, zinnia (Fig. 9B) showed complete removal of styrene after treatment with 1 g/kg of nZVI, nZVI-AC, T-nZVI-AC, or B-nZVI. However, styrene removal efficiencies of sunn hemp (Fig. 9A), zinnia (Fig. 9B), and marigold (Fig. 9C) without nZVI and carbon-based nZVI were 30%, 67%, and 56%, respectively. Statistical analysis (ANOVA) revealed that removal efficiencies differed significantly from those of the control (styrene-contaminated soil). Adding nZVI to styrene-contaminated soil improved the removal efficiency by approximately 20–50%, depending on the plant species. The integration of green nanotechnology and carbon-based materials has played a major role in the growth of plants and the enhancement of the remediation of soil contaminated with organic chemicals [14]. Although nZVI-AC does not provide the soil with nutrients, its application cannot solve the deficit of nutrients or organic matter; however, it can stabilize toxic substances such as pesticides and heavy metals in the soil [48]. Moreover, when activated carbon is mixed with soil, the soil density can be decreased and the porosity and field water capacity can be increased [49]. The high porosity and large surface area of carbon-based materials make them excellent habitats for beneficial microorganisms, such as bacteria and fungi, which help in nutrient cycling and plant growth [50]. In addition, the presence of certain nanoparticles, particularly nZVI, can improve the antioxidant status of plants, enhancing their capacity to withstand harsh conditions [51]. However, nanoparticles in soils may alter soil pH, affecting various properties, such as the accessibility of nutrients in the soil, microbial dynamics, and plant development and growth [52]. In the present study, the soil pH ranged from 5.5 to 6.7. Moreover, the application of low nZVI concentrations promoted phytoremediation using *Lolium perenne,* whereas high nZVI concentrations inhibited plant growth and oxidative stress [53].

After 28 days, the biomass of each plant in all treatments was investigated. Plant growth was stunted in comparison with plants growing in clean soil. With the same removal efficiency (100%), the biomass of sunn hemp in nano-phytoremediation treatments differed by approximately 0.31–1.60 g, whereas the biomass of zinnia differed by 0.99–10.68 g, compared with that of the control experiment. For marigold, the difference in biomass was only 2.40–8.85 g (Fig. S3). The cross-sections of marigold growing in the control, styrene-contaminated soil, and nano-phytoremediation treatment were examined under a microscope (Fig. S4). Comparing the roots, stems, and leaves of marigold, there were significant changes in the stomatal response to styrene in this study. Based on a literature review, the toxicological effects of styrene on plants have been discussed and clarified [54]. However, there was a distinct reduction in the height of plants and the yield of dry matter caused by styrene. Moreover, the number of stomata on the leaf surface decreased, and inhibition of assimilation and water use efficiency in the photosynthesis process were also detected in plants exposed to higher levels of styrene vapors [42]. The results confirm that styrene and styrene degradation may affect plant growth and development.

In addition, the leaves, stems, and roosts of sunn hemp, zinnia, and marigold were analyzed to determine the amount of styrene in the tissues (Fig. S5). The results showed that styrene was present in sunn hemp and zinnia. The styrene concentrations in zinnia roots were ranged from 0.14 to 0.25 mg/g. Meanwhile, styrene was not detected in the roots of sunn hemp and marigold in all treatments. Moreover, styrene was also found in the stems of zinnia, ranging between 0.02 mg/g and 0.04 mg/g. Meanwhile, styrene was not detected in the stems of sunn hemp and marigold. Small amounts of styrene were found in the leaves of zinnia (0.01–0.03 mg/g), while a high styrene concentration was found in the leaves of sunn hemp (0.03–0.14 mg/g). However, styrene has also been detected in marigolds. Styrene may be volatilized from stems or leaves (direct phytovolatilization), or from the soil owing to plant root activities (indirect phytovolatilization) [55]. The transport of volatile organic compounds (VOCs), including styrene, to plant tissues can also occur via diffusion, as VOCs diffuse through the water and air spaces in plant stems and trunks [56]. Doucette et al. (2013) studied trichloroethylene volatilization from leaves, trunks, and soil to assess the significance of these pathways in phytoremediation [57]. They found that volatilization primarily occurred through the soil. In our nano-phytoremediation, the addition of carbon-based nZVI improved aeration in the soil and increased vapor fluxes to the subsurface and root zones of plants. Root turnover can lead to the creation of low-tortuosity pathways that enhance contaminant volatilization [55]. However, a previous study showed that lower amounts of the pesticide chlorfenapyr accumulated in the roots and leaves of *Plantago major* during nano-phytoremediation [14]. This is because the degradation of nZVI without carbon-based ligands in water reduces the uptake of pollutants by the roots and leaves. Therefore, enhancing the pollutant dissipation rate in phytoremediation systems is necessary for nano-phytoremediation. In the current study, marigold was an alternative plant for the nano-phytoremediation of styrene-contaminated soil owing to its sturdy

nature, high biomass, tolerance to toxic effects, and ease of cultivation [47].

Nano-phytoremediation offers substantial environmental benefits, requiring limited energy, material consumption, and CO_2 sequestration (O'Connor et al., 2019). However, sustainable nano-phytoremediation depends on variety of meteorological parameters; therefore, it is crucial to identify and use environmentally stable nanomaterials [58]. Using life cycle assessment software (SigmaPro (free trial)), the life cycle of this green remediation was divided into five stages: manufacturing of AC and green-synthesized nZVI, transportation, construction and installation, operation and maintenance, and decommissioning and disposal for plants. Remediation of 1 cubic meter of styrene-contaminated soil by a combination of carbon-based nanoscale zero-valent iron and phytoremediation by marigolds (*Tagetes erecta* L.) emitted 0.0027 $tkgCO_2/m^3$ (Table S2) and biomass was around 6 kg/m^3 soil. The biomass to carbon conversion factor of 0.5 used is a good approximation of the typical carbon content in the biomass of terrestrial vegetation by IPCC (2003), so the carbon stock for this remediation method is 34 kgC/m^3 [59]. Previous research estimated carbon dioxide emission from various remediation methods. Lanari et al. (2014) indicated carbon dioxide emission from bioremediation of BTEX-contaminated soil was 0.00232 $tkgCO_2/m^3$ whereas 0.055 $tkgCO_2/m^3$ was produced from bioremediation of hydrocarbon-contaminated soil [60,61]. In addition, high carbon dioxide was released from physical/chemical remediation of organic chemicals, for example, soil vapor extraction (0.422 $tkgCO_2/m^3$) and excavation and disposal (0.012 $tkgCO_2/m^3$) [61,62].

4. Conclusion

Styrene contamination of the environment is harmful to public health and requires urgent restoration. All three carbon-based nanoscale zero-valent iron, nZVI-AC, T-nZVI-AC, and B-nZVI-AC were able to remove 100% of styrene at 72 h in water and >60% at 28 h in soil. Our results also indicated the intermediates of styrene possible were styrene oxide and 1-phenylethane-1,2-diol Moreover, adding carbon-based nZVI was able to enhance phytoremediation by *sunn hemp (C. juncea), zinnia (Z. violacea* Cav.*), and marigolds (T. erecta* L.*)*. The removal efficiency of styrene in soil was 100% by 28 h. The removal mechanisms of styrene from soil involved the adsorption of styrene on iron oxide shell on nZVI and on AC, indirect oxidation by nZVI, and phytovolatilization by plants. However, due to the physico-chemical properties of styrene, 25% of styrene in contaminated soil was removed by leaching, run off, volatilization, and naturally. In addition, styrene and its degradation products are phytotoxic to plants and affect their growth and development. To use this nano-phytoremediation technology, it is necessary to select suitable plants that are strong in nature, tolerant to toxic effects, easy to cultivate, non-attractive to herbivores, and have high absorption capacity and biomass.

Funding statement

This research project was supported by a grant from the Fundamental Fund FF: Basic Research (KU in fiscal year 2566 FF(KU)19.66. We are grateful for the support from the Kasetsart University Research and Development Institute (KURDI, Kasetsart Universityy, Bangkok, Thailand.

Additional Information

Supplementary material related to this article was added at separated file.

Data availability statement

The authors declare that the data supporting the findings of this study are available within the paper, a request for more detailed data should be sent to the corresponding authors with the permission of all authors.

CRediT authorship contribution statement

Ann Kambhu: Formal analysis, Data curation. **Tunlawit Satapanajaru:** Writing – review & editing, Writing – original draft, Supervision, Resources, Project administration, Methodology, Funding acquisition, Conceptualization. **Piyapawn Somsamak:** Data curation. **Patthra Pengthamkeerati:** Data curation. **Chanat Chokejaroenrat:** Data curation. **Kanitchanok Muangkaew:** Investigation. **Kanthika Nonthamit:** Investigation.

Declaration of competing interest

The authors declare that they have no known competing financial interests or personal relationships that could have appeared to influence the work reported in this paper.

Acknowledgments

This research project was supported by a grant from the Fundamental Fund FF: Basic Research (KU in fiscal year 2566 FF(KU)19.66. This research was funded by Kasetsart University Research and Development Institute (KURDI), Kasetsart University, Bangkok, Thailand. We are grateful for providing all scientific equipment from Department of Environmental Technology and Management, Faculty of Environment, Kasetsart University, Bangkok, Thailand.

Appendix A. Supplementary data

Supplementary data to this article can be found online at https://doi.org/10.1016/j.heliyon.2024.e27499.

References

[1] IARC, Agents classified by the IARC monographs, volumes vols. 1–132. Accessed: Mar. 07, 2023. [Online]. Available: https://monographs.iarc.who.int/list-of-classifications.

[2] US EPA, TRI Factsheet for Chemical Styrene, 0000100425 | TRI Explorer, US EPA, 2021. Accessed: Mar. 07, 2023. [Online], https://enviro.epa.gov/triexplorer/chemical.html?pYear=2021&pLoc=0000100425&pParent=TRI&pDataSet=TRIQ1.

[3] N. Colombani, M. Mastrocicco, A. Gargini, G.B. Davis, H. Prommer, Modelling the fate of styrene in a mixed petroleum hydrocarbon plume, J. Contam. Hydrol. 105 (2009) 38–55, https://doi.org/10.1016/J.JCONHYD.2008.11.005.

[4] W.R. Roy, R.A. Griffin, Mobility of organic solvents in water-saturated soil materials, Environ. Geol. Water Sci. 7 (1985) 241–247, https://doi.org/10.1007/BF02509925.

[5] T. Satapanajaru, C. Chokejaroenrat, C. Sakulthaew, M. Yoo-iam, Remediation and Restoration of petroleum hydrocarbon containing Alcohol-contaminated soil by persulfate oxidation activated with soil minerals, Water Air Soil Pollut. 228 (2017) 345, https://doi.org/10.1007/s11270-017-3527-x.

[6] M.H. Fu, M. Alexander, Biodegradation of styrene in samples of natural environments, Environ. Sci. Technol. 26 (1992) 1540–1544, https://doi.org/10.1021/ES00032A007/ASSET/ES00032A007.FP.PNG_V03.

[7] M. Oelschlägel, J. Zimmerling, D. Tischler, A review: the styrene metabolizing cascade of side-chain oxygenation as biotechnological basis to gain various valuable compounds, Front. Microbiol. 9 (2018) 490, https://doi.org/10.3389/FMICB.2018.00490/BIBTEX.

[8] N.D. O'Leary, K.E. O'Connor, A.D.W. Dobson, Biochemistry, genetics and physiology of microbial styrene degradation, FEMS Microbiol. Rev. 26 (2002) 403–417, https://doi.org/10.1111/J.1574-6976.2002.TB00622.X.

[9] A. Muratova, T. Hübner, S. Tischer, O. Turkovskaya, M. Möder, P. Kuschk, Plant–rhizosphere-microflora association during phytoremediation of PAH-contaminated soil, Int. J. Phytoremediation 5 (2003) 137–151, https://doi.org/10.1080/713610176.

[10] Y. Teng, Y. Shen, Y. Luo, X. Sun, M. Sun, D. Fu, Z. Li, P. Christie, Influence of Rhizobium meliloti on phytoremediation of polycyclic aromatic hydrocarbons by alfalfa in an aged contaminated soil, J. Hazard Mater. 186 (2011) 1271–1276, https://doi.org/10.1016/J.JHAZMAT.2010.11.126.

[11] W. Liang, et al., Recent advances of carbon-based nano zero valent iron for heavy metals remediation in soil and water: a critical review, J. Hazard Mater. 426 (2022) 127993, https://doi.org/10.1016/j.jhazmat.2021.127993.

[12] T. Satapanajaru, P. Anurakpongsatorn, A. Songsasen, H. Boparai, J. Park, Using low-cost iron byproducts from automotive manufacturing to remediate DDT, Water, Air, and Soil Pollution 175 (2006) 361–374, https://doi.org/10.1007/S11270-006-9143-9/METRICS.

[13] A.A. Romeh, R.A. Ibrahim Saber, Green nano-phytoremediation and solubility improving agents for the remediation of chlorfenapyr contaminated soil and water, J Environ Manage 260 (2020) 110104, https://doi.org/10.1016/j.jenvman.2020.110104.

[14] A.M. Abdelfatah, M. Fawzy, A.S. Eltaweil, M.E. El-Khouly, Green synthesis of nano-zero-valent iron using Ricinus communis seeds extract: Characterization and application in the treatment of methylene blue-polluted water, ACS Omega 6 (2021) 25397–25411, https://doi.org/10.1021/acsomega.1c03355.

[15] A.A. Romeh, R.A. Ibrahim Saber, Green nano-phytoremediation and solubility improving agents for the remediation of chlorfenapyr contaminated soil and water, J. Environ. Manag. 260 (2020) 110104, https://doi.org/10.1016/J.JENVMAN.2020.110104.

[16] S.P. Chandran, M. Chaudhary, R. Pasricha, A. Ahmad, M. Sastry, Synthesis of Gold Nanotriangles and Silver nanoparticles using Aloevera plant extract, Biotechnol. Prog. 22 (2006) 577–583, https://doi.org/10.1021/BP0501423.

[17] T. Bhuyan, K. Mishra, M. Khanuja, R. Prasad, A. Varma, Biosynthesis of zinc oxide nanoparticles from Azadirachta indica for antibacterial and photocatalytic applications, Mater. Sci. Semicond. Process. 32 (2015) 55–61, https://doi.org/10.1016/J.MSSP.2014.12.053.

[18] S. Jadoun, R. Arif, Nirmala, K. Jangid, Rajesh, K. Meena, Green synthesis of nanoparticles using plant extracts: a review, Environ. Chem. Lett. 19 (2021) 355–374, https://doi.org/10.1007/s10311-020-01074-x.

[19] F. Zhu, Y. Yang, W. Ren, R.M. Iribagiza, W. Wang, Coupling electrokinetic remediation with flushing using green tea synthesized nano zero-valent iron/nickel to remediate Cr (VI), Environ. Geochem. Health 45 (2023) 9691–9707, https://doi.org/10.1007/s10653-023-01767-6.

[20] F. Zhu, Y. Wu, Y. Liang, H. Li, W. Liang, Degradation mechanism of norfloxacin in water using persulfate activated by BC@nZVI/Ni, Chem. Eng. J. 389 (2020) 124276, https://doi.org/10.1016/j.cej.2020.124276.

[21] Y. Rashtbari, F. Sher, S. Afshin, A. Hamzezadeh bahrami, S. Ahmadi, O. Azhar, A. Rastegar, S. Ghosh, Y. Poureshgh, Green synthesis of zero-valent iron nanoparticles and loading effect on activated carbon for furfural adsorption, Chemosphere 287 (2022) 132114, https://doi.org/10.1016/J.CHEMOSPHERE.2021.132114.

[22] D.W. Nelson, L.E. Sommers, Total carbon, organic carbon, and organic matter, in: D.L. Sparks, A.L. Page, P.A. Helmke, R.H. Loeppert, P.N. Soltanpour, M. A. Tabatabai, C.T. Johnston, M.E. Sumner (Eds.), Methods of Soil Analysis, Part 3: Chemical Methods, John Wiley & Sons, Ltd, 1996, pp. 961–1010, https://doi.org/10.2136/SSSABOOKSER5.3.C34.

[23] J.D. Rhoades, Cation exchange capacity, in: R.H. Buxton, D.R. Miller Keeney (Eds.), Methods of Soil Analysis, 1982, pp. 149–158. Madison.

[24] T. Satapanajaru, C. Chompuchan, P. Suntornchot, P. Pengthamkeerati, Enhancing decolorization of Reactive Black 5 and Reactive Red 198 during nano zerovalent iron treatment, Desalination 266 (2011) 218–230, https://doi.org/10.1016/j.desal.2010.08.030.

[25] D. Wang, P. Yang, Y. Zhu, Growth of Fe3O4 nanoparticles with tunable sizes and morphologies using organic amine, Mater. Res. Bull. 49 (2014) 514–520, https://doi.org/10.1016/j.materresbull.2013.09.019.

[26] D. Lin, L. Hu, I.M.C. Lo, Z. Yu, Size distribution and Phosphate removal capacity of nano zero-valent iron (nZVI): influence of pH and ionic Strength, Water 12 (2020) 2939, https://doi.org/10.3390/w12102939.

[27] S. Saif, A. Tahir, Y. Chen, Green synthesis of iron nanoparticles and their environmental applications and Implications, Nanomaterials 6 (2016) 209, https://doi.org/10.3390/nano6110209.

[28] S. V Ganachari, J.S. Yaradoddi, S.B. Somappa, P. Mogre, R.P. Tapaskar, B. Salimath, A. Venkataraman, V.J. Viswanath, Green nanotechnology for Biomedical, Food, and agricultural applications, in: L.M.T. Martínez, O.V. Kharissova, B.I. Kharisov (Eds.), Handbook of Ecomaterials, Springer International Publishing, Cham, 2019, pp. 2681–2698, https://doi.org/10.1007/978-3-319-68255-6_184.

[29] S. Mortazavian, H. An, D. Chun, J. Moon, Activated carbon impregnated by zero-valent iron nanoparticles (AC/nZVI) optimized for simultaneous adsorption and reduction of aqueous hexavalent chromium: material characterizations and kinetic studies, Chem. Eng. J. 353 (2018) 781–795, https://doi.org/10.1016/j.cej.2018.07.170.

[30] J. Li, C. Chen, K. Zhu, X. Wang, Nanoscale zero-valent iron particles modified on reduced graphene oxides using a plasma technique for Cd(II) removal, J. Taiwan Inst. Chem. Eng. 59 (2016) 389–394, https://doi.org/10.1016/j.jtice.2015.09.010.

[31] Y.X. Huang, J. Guo, C. Zhang, Z. Hu, Hydrogen production from the dissolution of nano zero valent iron and its effect on anaerobic digestion, Water Res. 88 (2016) 475–480, https://doi.org/10.1016/j.watres.2015.10.028.

[32] F. Corvaisier, Y. Schuurman, A. Fecant, C. Thomazeau, P. Raybaud, H. Toulhoat, D. Farrusseng, Periodic trends in the selective hydrogenation of styrene over silica supported metal catalysts, J. Catal. 307 (2013) 352–361, https://doi.org/10.1016/j.jcat.2013.08.009.

[33] M.M. Tarekegn, A.M. Hiruy, A.H. Dekebo, Correction: nano zero valent iron (nZVI) particles for the removal of heavy metals (Cd2+, Cu2+ and Pb2+) from aqueous solutions, RSC Adv. 11 (2021) 27084, https://doi.org/10.1039/D1RA90135D.

[34] H.K. Boparai, M. Joseph, D.M. O'Carroll, Kinetics and thermodynamics of cadmium ion removal by adsorption onto nano zerovalent iron particles, J. Hazard Mater. 186 (2011) 458–465, https://doi.org/10.1016/j.jhazmat.2010.11.029.
[35] S. Nam, P. Tratnyek, Reduction of Azo dyes with zero-valent iron, Water Res. 34 (2000) 1837–1845, https://doi.org/10.1016/S0043-1354(99)00331-0.
[36] L. Xie, H. Wang, B. Lu, J. Zhao, Q. Cai, Highly selective oxidation of styrene to benzaldehyde over Fe3O4 using H2O2 aqueous solution as oxidant, React. Kinet. Mech. Catal. 125 (2018) 743–756, https://doi.org/10.1007/s11144-018-1429-6.
[37] A.P.S. Oliveira, I.S. Gomes, A.C. Oliveira, J.M. Filho, G.D. Saraiva, J.M. Soares, F.F. de Sousa, A. Campos, Styrene oxidation to valuable compounds over Nanosized FeCo-based catalysts: effect of the Third metal addition, Catalysts 7 (2017) 323, https://doi.org/10.3390/catal7110323.
[38] P.J. McCall, D.A. Laskowski, R.L. Swann, H.J. Dishburger, Measurement of sorption coefficients of organic chemicals and their use, in environmental fate analysis, in: Test Protocols for Environmental Fate and Movement of Toxicants. Proceedings of AOAC Symposium, AOAC., 1981, pp. 89–109.
[39] R.J. Parod, Styrene, in: P. Wexler (Ed.), Encyclopedia of Toxicology, third ed., Academic Press, Oxford, 2014, pp. 409–412, https://doi.org/10.1016/B978-0-12-386454-3.00065-8.
[40] M.I. Banton, S.S. Sarang, Styrene, in: P. Wexler (Ed.), Encyclopedia of Toxicology, fourth ed., Academic Press, Oxford, 2024, pp. 763–774, https://doi.org/10.1016/B978-0-12-824315-2.00422-X.
[41] T. Vaithiyanathan, P. Sundaramoorthy, Analysis of sugar mill effluent and its influence on germination and growth of African marigold (Tagetes erecta L.), Appl. Water Sci. 7 (2017) 4715–4723, https://doi.org/10.1007/s13201-017-0634-1.
[42] A. Stolarska, K. Przybulewska, A. Wieczorek, A. Gregorczyk, Physiological activity of Wheat cv. Tonacja seedlings as affected by chemical stress of styrene Vapours, Pol. J. Environ. Stud. 19 (2010) 789–796.
[43] P. Mañas, J. De las Heras, Phytotoxicity test applied to sewage sludge using Lactuca sativa L. and Lepidium sativum L. seeds, Int. J. Environ. Sci. Technol. 15 (2017) 273–280, https://doi.org/10.1007/s13762-017-1386-z.
[44] J.K. Adesodun, M.O. Atayese, T.A. Agbaje, B.A. Osadiaye, O.F. Mafe, A.A. Soretire, Phytoremediation potentials of Sunflowers (Tithonia diversifolia and Helianthus annuus) for metals in soils contaminated with zinc and lead Nitrates, Water Air Soil Pollut. 207 (2009) 195–201, https://doi.org/10.1007/s11270-009-0128-3.
[45] M. Sakakibara, Y. Ohmori, N.T.H. Ha, S. Sano, K. Sera, Phytoremediation of heavy metal-contaminated water and sediment by Eleocharis acicularis, CLEAN – soil, Air, Water 39 (2011) 735–741, https://doi.org/10.1002/clen.201000488.
[46] N. Shabani, M.H. Sayadi, Evaluation of heavy metals accumulation by two emergent macrophytes from the polluted soil: an experimental study, Environmentalist 32 (2012) 91–98, https://doi.org/10.1007/s10669-011-9376-z.
[47] A. Kafle, A. Timilsina, A. Gautam, K. Adhikari, A. Bhattarai, N. Aryal, Phytoremediation: mechanisms, plant selection and enhancement by natural and synthetic agents, Environmental Advances 8 (2022) 100203, https://doi.org/10.1016/j.envadv.2022.100203.
[48] D. Baragano, R. Forjan, N. Alvarez, J.R. Gallego, A. Gonzalez, Zero valent iron nanoparticles and organic fertilizer assisted phytoremediation in a mining soil: Arsenic and mercury accumulation and effects on the antioxidative system of Medicago sativa L, J. Hazard Mater. 433 (2022) 128748, https://doi.org/10.1016/j.jhazmat.2022.128748.
[49] J. Gao, D. Liu, Y. Xu, J. Chen, Y. Yang, D. Xia, Y. Ding, W. Xu, Effects of two types of activated carbon on the properties of vegetation concrete and Cynodon dactylon growth, Sci. Rep. 10 (2020) 14483, https://doi.org/10.1038/s41598-020-71440-w.
[50] K. Dawar, et al., Evaluating the Efficacy of activated carbon in Minimizing the Risk of heavy metals contamination in Spinach for safe consumption, ACS Omega 8 (2023) 24323–24331, https://doi.org/10.1021/acsomega.3c01573.
[51] P. Prakash, S.C. S, Nano-phytoremediation of heavy metals from soil: a critical review, Pollutants 3 (2023) 360–380, https://doi.org/10.3390/pollutants3030025.
[52] F. Fernandez, R. Hoeft, Managing Soil pH and Crop Nutrients, Illinois Agronomy Handbook, 2009, pp. 91–112.
[53] D. Huang, et al., Nanoscale zero-valent iron assisted phytoremediation of Pb in sediment: impacts on metal accumulation and antioxidative system of Lolium perenne, Ecotoxicol. Environ. Saf. 153 (2018) 229–237, https://doi.org/10.1016/j.ecoenv.2018.01.060.
[54] B.F. Gibbs, C.N. Mulligan, Styrene toxicity: an Ecotoxicological assessment, Ecotoxicol. Environ. Saf. 38 (1997) 181–194, https://doi.org/10.1006/eesa.1997.1526.
[55] M. Limmer, J. Burken, Phytovolatilization of organic contaminants, Environ. Sci. Technol. 50 (2016) 6632–6643, https://doi.org/10.1021/acs.est.5b04113.
[56] M.C. Reid, P.R. Jaffe, A push-pull test to measure root uptake of volatile chemicals from wetland soils, Environ. Sci. Technol. 47 (2013) 3190–3198, https://doi.org/10.1021/es304748r.
[57] W. Doucette, H. Klein, J. Chard, R. Dupont, W. Plaehn, B. Bugbee, Volatilization of trichloroethylene from trees and soil: measurement and scaling approaches, Environ. Sci. Technol. 47 (2013) 5813–5820, https://doi.org/10.1021/es304115c.
[58] Z. Gul, S. Ullah, S. Khan, H. Ullah, M.U. Khan, M. Ullah, S. Ali, A.A. Altaf, Recent Progress in nanoparticles based Sensors for the detection of mercury (II) ions in environmental and biological samples, Crit. Rev. Anal. Chem. 54 (2024) 44–60, https://doi.org/10.1080/10408347.2022.2049676.
[59] IPCC, Good Practice Guidance for Land Use, Land-Use Change and Forestry, Institute for Global Environmental Strategies (IGES), 2003 [Online], https://www.ipcc-nggip.iges.or.jp/public/gpglulucf/gpglulucf_files/0_Task1_Cover/Cover_TOC.pdf.
[60] C. Lanari, P. Ambrosini, L. Patata, G. Crimi, P. Ragni, P. Schillaci, Remediation of gas stations: sustainability assessment of Excavation and removal of contaminated soil (Tools, Metrics and Indicators), in: The 3rd International Conference on Sustainable Remediation, 2014. Accessed: Feb. 29, 2024. [Online]. Available: https://dokumen.tips/documents/remediation-of-gas-stations-sustainability-assessment-23-ambrosinipaolo183pdf.html?page=1.
[61] R.T. Gill, S.F. Thornton, M.J. Harbottle, J.W.N. Smith, Sustainability assessment of electrokinetic bioremediation compared with alternative remediation options for a petroleum release site, J. Environ. Manag. 184 (2016) 120–131, https://doi.org/10.1016/j.jenvman.2016.07.036.
[62] Y. Choi, J.M. Thompson, D. Lin, Y.M. Cho, N.S. Ismail, C.H. Hsieh, R.G. Luthy, Secondary environmental impacts of remedial alternatives for sediment contaminated with hydrophobic organic contaminants, J. Hazard Mater. 304 (2016) 352–359, https://doi.org/10.1016/J.JHAZMAT.2015.09.069.